Allosteric modulation by sodium ions and amilorides of G protein-coupled receptors : a closer look at the sodium ion site of the adenosine A2a receptor and development of a mass spectrometry ligand binding assay for adenosine A1 and A2a receptors

Massink, A.

Chapter 3

The role of a sodium ion binding site in the allosteric modulation of the A_{2A} adenosine G protein-coupled receptor

Hugo Gutiérrez-de-Terán*
Arnault Massink*
David Rodríguez
Wei Liu
Gye Won Han
Jeremiah S. Joseph
Ilia Katritch
Laura H. Heitman
Lizi Xia
Adriaan P. IJzerman
Vadim Cherezov
Vsevolod Katritch
Raymond C. Stevens

**These authors contributed equally*

Structure, 2013, 21(12): 2175-85

Abstract

The function of G protein-coupled receptors (GPCRs) can be modulated by a number of endogenous allosteric molecules. In this study, we used molecular dynamics, radioligand binding and thermostability experiments to elucidate the role of the recently discovered sodium ion binding site in the allosteric modulation of the human A_{2A} adenosine receptor, conserved among class A GPCRs. While the binding of antagonists and sodium ions to the receptor was noncompetitive in nature, the binding of agonists and sodium ions appears to require mutually exclusive conformational states of the receptor. Amiloride analogs can also bind to the sodium binding pocket, showing distinct patterns of agonist and antagonist modulation. These findings suggest that physiological concentrations of sodium ions affect functionally relevant conformational states of GPCRs, and can help to design novel synthetic allosteric modulators or bitopic ligands exploiting the sodium ion binding pocket.

Introduction

Cellular responses to a wide variety of extracellular signals are mediated by the superfamily of seven transmembrane helical receptors coupled to intracellular G proteins (G protein-coupled receptors, GPCRs). It is now well recognized that many GPCRs function as "allosteric machines" with the orthosteric binding pocket representing just one of the many sites for possible signal modulation and pharmacological intervention. Thus, molecules targeting other (allosteric) sites can modulate binding of native orthosteric ligands and shift the delicate equilibrium between active and inactive states of GPCRs.[1] Potential therapeutic advantages include a gain in target selectivity, the "ceiling effect", and preservation of the spatiotemporal profile of intercellular signaling.[2-5] Some endogenous chemical entities, such as ions or lipids, have also been demonstrated to act as allosteric modulators of GPCRs,[1, 6, 7] but the structural basis and functional importance of these interactions are not well understood.

Recent advances in protein engineering and membrane protein crystallography[8-10] have led to the elucidation of a growing number of experimental GPCR structures,[11] contributing to the alluring perspective of structure-based drug design,[12] and the deciphering of molecular mechanisms underlying conformational equilibrium.[13] Several receptors, including one of the best-characterized GPCRs, the A_{2A} adenosine receptor (A_{2A}AR), have been crystallized in inactive[14-17] and active-like[18, 19] conformations. The conformational changes associated with A_{2A}AR activation mirrored similar structural changes observed in other receptors, namely the β_2-adrenergic receptor (β_2AR)[20] and rhodopsin.[21] Recently, the 1.8 Å resolution structure of inactive A_{2A}AR in complex with ZM-241,385 revealed the presence of a sodium ion bound to the core of the transmembrane (TM) bundle,[22] coordinated by $Asp^{2.50}$ and other side chains highly conserved in class A GPCRs[23] and by a cluster of structural water molecules.[24, 25] The allosteric effect of sodium ions has been described previously in A_{2A} and A_1 adenosine receptors,[6, 26] as well as in GPCRs from other subfamilies such as dopamine D_2,[7, 27] opioid,[28, 29] or α-adrenergic receptors,[30, 31] among others. Similarly, the positively charged, synthetic small molecule amiloride and its analogs have been found to be allosteric modulators of agonist and antagonist binding of a number of GPCRs (Chapter 2), including A_{2A}AR, and were shown to compete with sodium ions for the same binding site.[6] Moreover, mutation of $Asp^{2.50}$ to either asparagine or alanine has been shown to reduce or abrogate the allosteric effects of

sodium ions or amiloride in many GPCRs.[7, 32-34] While the 1.8 Å structure of A_{2A}AR provides a static picture of sodium interactions with the receptor, the dynamic nature of the sodium ion-water cluster, its effect on binding of orthosteric agonists and antagonists, and its functional role are poorly understood. Molecular dynamics (MD) studies, supported by biochemical and biophysical experiments, provide a molecular framework for the allosteric effects of sodium and amilorides, which can ultimately aid in the discovery of new compounds targeting this site.[4]

Material and methods

Computational simulations

The standard amino acid sequence numbering for the human A_{2A}AR is used in the text, with the Ballesteros and Weinstein residue numbering for GPCRs[35] shown in superscript if the residue belongs to a transmembrane helix. The inactive structure of the A_{2A}AR in complex with ZM-241,385 and a sodium ion (PDB code 4EIY),[22] was refined in order to model the missing loops and add protons as detailed in the supplemental information, prior to MD simulations. When the sodium ion was not considered, manual replacement with a water molecule, also maintaining the surrounding water molecules, was followed by energy minimization to fully optimize the H-bond network in the allosteric site. In the simulations with amiloride, the initial conformation of the A_{2A}AR-amiloride complex was used as proposed previously by flexible docking.[22] The starting coordinates of the antagonist caffeine were obtained by superimposing the A_{2A}AR-caffeine complex (PDB code 3RFM)[14] with the A_{2A}AR structure described above using PyMOL (The PyMOL Molecular Graphics System version 1.4, Schrödinger). The MD simulations of the active-like conformation were performed starting from the A_{2A}AR in complex with the stabilizing agonist UK-432,097 (PDB code 3QAK).[19] The starting coordinates of the sodium ion and coordinating water molecules were transposed from the inactive structure by structural superimposition with 4EIY. Finally, the A_{2A}AR in complex with the agonist NECA was obtained by "morphing" the A_{2A}AR-ZM-241,385 structure (PDB code 4EIY) to the active-state A_{2A}AR-UK-432,097 conformation (PDB code 3QAK), and subsequent reconstruction of the intracellular loop 3 as detailed in the supplemental experimental procedures. Note that the available crystal structure of NECA in complex with thermostabilized A_{2A}AR (PDB code 2YDV),[18] was not suitable for this analysis because of a highly distorted conformation

of the allosteric site, which includes a deformed helix VII backbone due to a cis-Proline in the NPxxY motif.

Table 1. Setup of the different MD simulations reported in this work.

	Receptor Conformation	Ligand	Allosteric Modulator	Replicas, length
MDS1[a]	Inactive	ZM-241,385	Na^+	3x100 ns
MDS1-b[a]	Inactive	ZM-241,385	Na^+	3x100 ns
MDS2	Inactive	---	Na^+	3x100 ns
MDS3	Inactive	ZM-241,385	---	3x100 ns
MDS4	Inactive	---	---	3x100 ns
MDS5	Active	UK-432,097	Na^+	3x40 ns
MDS6	Active	NECA	Na^+	3x40 ns
MDS7	Active	---	Na^+	3x40 ns
MDS8	Inactive	ZM-241,385	Amiloride	3x100 ns
MDS9	Inactive	Caffeine	Amiloride	3x40 ns
MDS10	Inactive	Caffeine	---	3x40 ns
MDS11	Inactive	ZM-241,385	HMA	3x100 ns
MDS12	Inactive	Caffeine	HMA	3x40 ns

a: MDS1-b corresponds to the same system as MDS1, but considering the physiological saline concentration of 150mM.

Membrane insertion and all MD simulations were performed with the GROMACS software,[36] using our original protocol for the MD simulations of GPCRs[37] as adapted in the PyMemDyn program.[38] The final systems, consisting of approximately 50,000 atoms (~74% belong to solvent molecules, ~15% to lipids and ~11% to protein and ligand atoms), were energy minimized and equilibrated for a total of 5 ns, with specific details provided in the supplemental experimental procedures. The production phase of unrestrained MD simulations followed for 100 ns simulation time (shorter production times were considered in certain cases, see Table 1 and explanation in main text). MD simulations were performed under the OPLSAA force field,[39] with ligand parameters obtained with Macromodel,[40] lipid parameters adapted from Berger[41] together with the use of the half-ε double-pairlist method[42] and the SPC water model.[43] The periodic boundary conditions (PBC) were implemented with hexagonal prism-shaped boxes in the isobaric NPT ensemble, using a Nose-Hoover thermostat[44] with a target temperature of 310 K using.

Electrostatic interactions beyond a cutoff of 12 Å were estimated with the particle mesh Ewald (PME) method. All MD analyses were conducted with several GROMACS and VMD[45] utilities. Molecular superimpositions, trajectory visualizations and molecular images were performed with PyMOL.

Cell growth and transfection

HEK293T cells were grown in culture medium consisting of Dulbecco's modified Eagle's medium (DMEM) supplemented with 10% newborn calf serum (NCS), 50 µg/ml streptomycin and 50 IU/ml penicillin at 37 °C and 7% CO_2. Cells were subcultured twice a week at a ratio of 1:15 on 10 cm ø plates. Cells were transfected with the wild-type A_{2A}AR-plasmid (pcDNA3.1, 1 µg) using the calcium phosphate precipitation method.[46]

Membrane preparation

Cells were detached from plates 48 h after transfection by scraping them into 5 ml phosphate buffered saline (PBS), collected and centrifuged at 700 ×g (3000 rpm) for 5 min. Pellets derived from 50 plates (10 cm ø) were pooled and resuspended in 40 ml of ice-cold assay buffer (50 mM Tris-HCl supplemented with 5 mM $MgCl_2$, pH 7.4). An Ultra-Turrax was used to homogenize the cell suspension. Membranes and the cytosolic fraction were separated by centrifugation at 100,000 ×g (31,000 rpm) in a Beckman Optima LE-80K ultracentrifuge at 4 °C for 20 min. The pellet was resuspended in 20 ml of Tris buffer and the homogenization and centrifugation step was repeated. Assay buffer (10 ml) was used to resuspend the pellet and adenosine deaminase (ADA) was added (0.8 IU/ml) to break down endogenous adenosine. Membranes were stored in 250 µl aliquots at -80 °C. Membrane protein concentrations were measured using the BCA (bicinchoninic acid) method.[47]

Competition and saturation binding assays using HEK293T cell membranes

For competition binding experiments with [^{3}H]ZM-241,385 (46.6 Ci/mmol, ARC Inc, St. Louis, MO, USA), between 6 and 8 µg of membranes was used to ensure that total binding was less than 10% of the total radioactivity added to prevent radioligand depletion. For [^{3}H]NECA (16.3 Ci/mmol, Perkin Elmer, Groningen, The Netherlands) competition binding experiments between 18 and 25 µg of membranes were used for the experiments. Membrane aliquots were incubated in a total volume of 100 µl of assay buffer at 25 °C for 2 h. Radioligand displacement experiments were performed using five concentrations of

competing ligand (NaCl, amiloride or HMA (5-[N,N-hexamethylene]amiloride), all from Sigma Aldrich, Zwijndrecht, The Netherlands). [^{3}H]ZM-241,385 and [^{3}H]NECA were used at concentrations of ~ 4.0 nM and 15-20 nM, respectively. Nonspecific binding was determined in the presence of 100 µM CGS21680 (Ascent Scientific, Bristol, UK, for experiments with [^{3}H]ZM-241,385) or 10 µM ZM-241,385 (Ascent Scientific, Bristol, UK, for experiments with [^{3}H]NECA) and represented less than 15% of the total binding. For saturation experiments, total binding was determined at increasing concentrations of [^{3}H]ZM-241,385 (0.10-45 nM), in the absence or presence of ZM-241,385 (10 nM), NaCl (30 or 100 mM), amiloride (30 µM), or HMA (3 µM). In addition, unlabeled NECA (Ascent Scientific, Bristol, UK) was spiked with 25% [^{3}H]NECA resulting in final concentrations of 8.0 to 400 nM, in the absence or presence of ZM-241,385 (10 nM), NaCl (30 or 100 mM), amiloride (30 µM), or HMA (4 µM). Nonspecific binding was determined at three concentrations of radioligand and analyzed by linear regression. Incubations were terminated by rapid vacuum filtration to separate the bound and free radioligand through 96-well GF/B filter plates using a Filtermate-harvester (PerkinElmer Life Sciences). Filters were subsequently washed three times with ice-cold assay buffer. The filter-bound radioactivity was determined by scintillation spectrometry using the PE 1450 Microbeta Wallac Trilux scintillation counter (PerkinElmer Life Sciences).

Thermostability assays

The A_{2A}AR-BRIL-ΔC receptor construct was purified from *Spodoptera frugiperda* (*Sf*9) insect cells in the *apo* form as described previously,[22] except that KCl was used throughout purification instead of NaCl. N-(4-[7-diethylamino-4-methyl-3-coumarinyl]phenyl)-maleimide (CPM) dye (Invitrogen) was dissolved in DMSO (Sigma) at 4 mg/ml and stored at −80 °C. Before use, the CPM stock solution was thawed and diluted 1:40 in dye dilution buffer (10 mM HEPES pH 7.50, 10% glycerol, 0.05% dodecyl maltoside (DDM) (Anatrace)). The thermal denaturation assay was performed with a total volume of 200 µl per sample in a quartz fluorimeter cuvette (Starna Cells, Inc., Atascadero, CA) and an apparent relative Tm was obtained.[48] Receptor (4 µg) was diluted in assay buffer (10 mM HEPES pH 7.5, 0.05% DDM, 0.01% cholesterol hemisuccinate (CHS) (Sigma)) with and without different concentrations and combinations of NaCl, amiloride, and ZM-241,385 to a final volume of 200 µl. 5 µl of the diluted dye was added to the protein-containing assay solution and incubated for 30 min at 4 °C. The mixed solutions were transferred into cuvettes and

fluorescence data were collected by a Cary Eclipse spectrofluorometer (Varian, USA) with a temperature ramping rate of 2 °C/min. The excitation wavelength was 387 nm and the emission wavelength was 463 nm. All assays were performed over a temperature range starting from 20 °C to 90 °C.

Data analysis

The radioligand binding and thermostability data were processed with Prism 5 (GraphPad Software, San Diego, CA, USA). Statistical significance was assessed with a Student's t-test.

Results

Molecular dynamics studies

A series of MD simulations were designed to evaluate the functional role of the sodium ion in the A_{2A}AR, as summarized in Table 1. Three MD replicates of 40-100 ns length each were run for each setup, in order to increase the statistics of the sampling, with a total simulation time exceeding 2.8 μs. The effect of the sodium ion on the conformational equilibrium of the receptor was examined considering both the inactive and active-like conformation of the A_{2A}AR (simulations MDS1-MDS7). The influence of the orthosteric ligands in this process was examined by comparing the MD simulations with and without the antagonist ZM-241,385 (MDS1 and MDS2) or the agonists UK-432,097 and NECA (MDS5 through MDS7). In addition, the allosteric effect of amiloride and its derivative HMA in the antagonist-bound conformation was examined in MDS8 through MDS12, with two distinct chemotypes of antagonists (i.e., ZM-241,385 and caffeine).

The sodium binding site in the A_{2A}AR inactive conformation

In the high resolution crystal structure of inactive A_{2A}AR,[22] the sodium ion is directly coordinated by Asp52$^{2.50}$ and Ser91$^{3.39}$ (first shell residues) and three structured water molecules (Figure 1A). Water molecules also bridge interactions with residues in the second (Trp246$^{6.48}$ and Asn280$^{7.45}$), and the third shells (Thr88$^{3.36}$ and Ser281$^{7.46}$). Overall, the sodium ion/water binding pocket is formed by 15 out of the 34 amino acids that are conserved in the majority of non-olfactory class A GPCRs[23] and their conformation is similar in most GPCRs crystallized in the inactive state (Figure 1B-D).

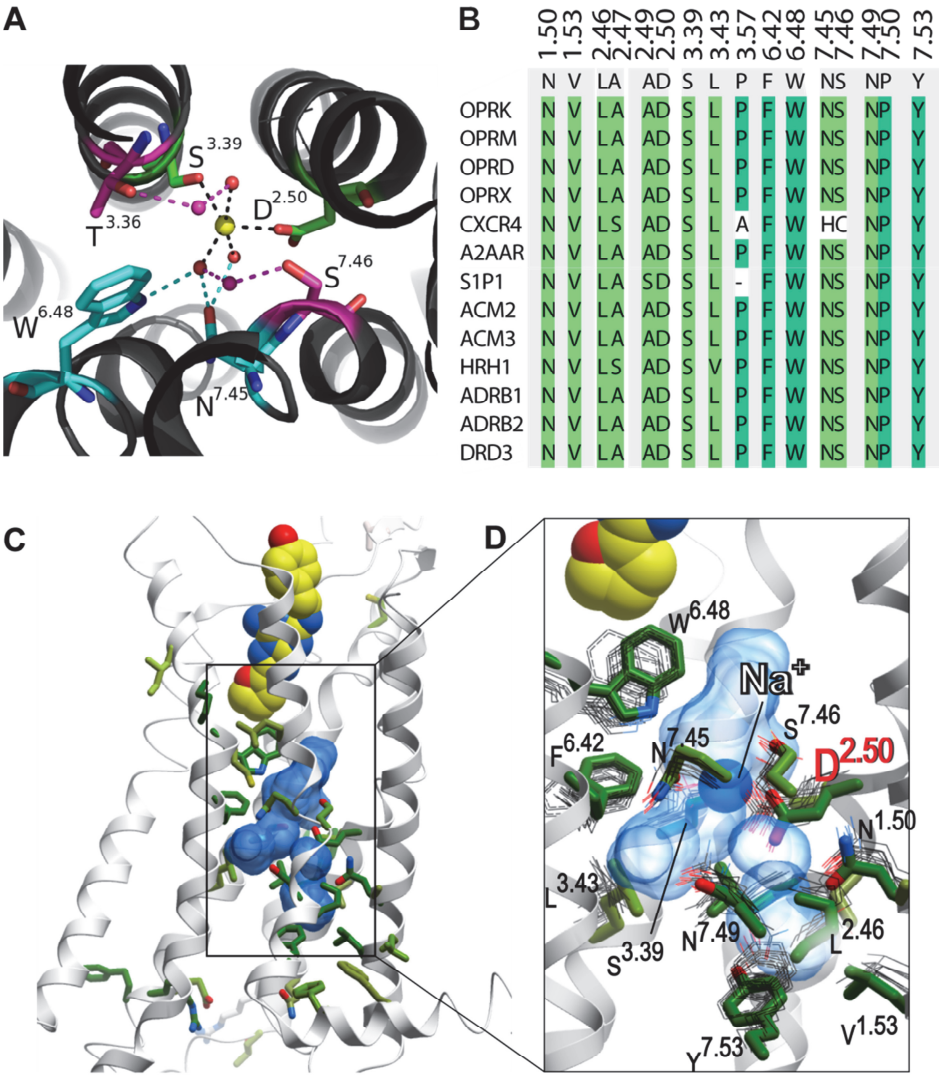

Figure 1. Structure and conservation of the central sodium ion-binding allosteric pocket in Class A GPCRs. **A)** The sodium ion distorted octahedral coordination as in the A_{2A}AR crystal structure: The first shell is occupied by two conserved polar residues (green) and three water molecules, which contact with a second shell of residues (cyan), or with a second layer of water molecules connecting with the third shell of residues (magenta). **B)** Sequence conservation of the 15 residues lining the binding pocket among inactive GPCR crystal structures. **C)** Structure of the A_{2A}AR complex with ZM-241,385, showing residues with higher than 50% conservation in all Class A receptors as sticks with green carbons. **D)** A close-up of the central allosteric pocket (transparent blue surface), showing the side chains located within 5 Å from the ten waters of the sodium ion-water cluster (green sticks: A_{2A}AR; gray thin lines: the corresponding side chains of the overlaid GPCR crystal structures listed in **B**. See also supplemental Figure S1.

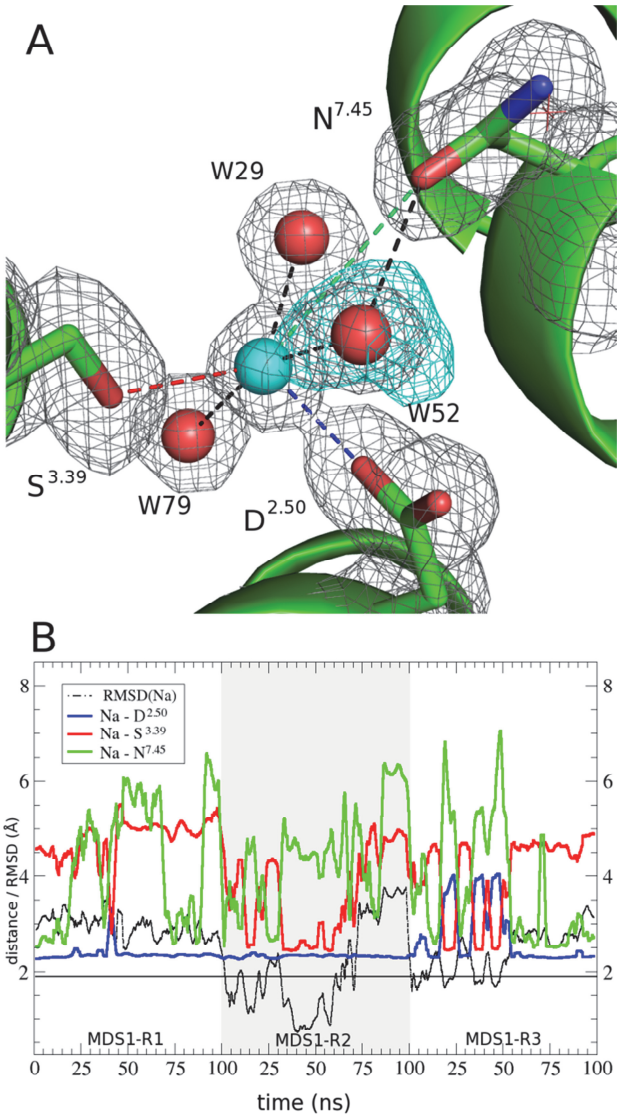

Figure 2. The two coordination states of the sodium ion as observed in MD simulations **A)** Volumetric density map (isosurface contoured at 0.3 $Å^{-3}$ value, blue) corresponding to the sodium ion occupancy as calculated from simulations MDS1 (see Table 1). The starting crystal structure is displayed, together with the electron density (contoured at 1 σ level, black). **B)** The time-evolution of the distances between the sodium ion and $Asp^{2.50}$ (blue), $Ser^{3.39}$ (red) and $Asn^{7.45}$ (green), shown for the 3 independent replicates (R1-R3) of MDS1. The corresponding distances are denoted as dashed lines in **A** with the same color code, and are the source of the data in Table S1. The RMSD of the ion with respect to its crystallographic position is indicated with a black line, while the horizontal bar at 1.8 Å (the resolution of the parent crystal structure) denotes the limit for the crystallographic coordination state (position c1). See also Table S1 and Figure S2.

Analysis of the sodium ion's mobility and its coordination state reveals a high level of stability for the ion when bound to the receptor's inactive conformation. The dominant charge-charge interaction with Asp52$^{2.50}$ is clearly maintained along the simulation runs in the different MD trajectories, while the side chain oxygen atoms of Ser91$^{3.39}$ and Asn280$^{7.45}$ alternate direct interactions with the ion (Figure 2). More precisely, the ion fluctuates between a coordination state as seen in the crystal structure, which we will refer to as position c1, and a second state that we will refer to as position c2. This fluctuation involves an exchange between the sodium ion and the water molecule W52, initially linked to the OD1 of Asn280$^{7.45}$, as shown in Figure 2A by the overlay of the electron density of the crystal structure with the volumetric density map calculated from the MD simulations. In position c2, the ion is still coordinated by Asp52$^{2.50}$ (OD1), while it is the OD1 of Asn280$^{7.45}$ (occasionally replaced by a new water molecule) that participates in the first coordination shell, which is completed with three other water molecules. The radial distribution function indicates the average sodium-oxygen distance is 2.4 Å, with the first coordination shell predominantly formed by 4 or 5 oxygen atoms (see supplemental Figure S2), in agreement with the geometric analysis of sodium ion binding sites found in the Protein Data Bank (PDB).[49] The consistent observation of these two dominant coordination modes suggests a possibility of fast exchange between the sodium ion and the water molecule, supported by the significantly shorter distance (2.2 Å) observed in the crystal structure for the Na^+-O(W52) pair. Interestingly, this fast exchange occurs regardless of the presence of the antagonist ZM-241,385 in the orthosteric binding site (Table S1). In the setup MDS1b, we evaluated the effects of a physiological saline concentration in the simulations, and observed no difference in results (see supplemental Figure S2 and Table S1). Moreover, none of the sodium ions from the extracellular solvent could cross the narrow channel into the allosteric pocket during 100 ns simulations, suggesting that exchange of sodium ions in A_{2A}AR may occur on a longer time scale.

To investigate a possible effect of the sodium ion on the stability of the inactive conformation of the receptor, the MD simulations described above (MDS1 and MDS2) were compared with the corresponding simulations of the inactive A_{2A}AR in the absence of the ion (MDS3 and MDS4). The most pronounced difference in local conformational dynamics was located in the region of the sodium ion: the highly conserved residue Trp246$^{6.48}$ in the second sphere of solvation experienced a rotameric transition from

theinitial *g+* rotamer to the *trans* (*t*) conformation, observed in two out of three independent simulations of the *apo* receptor without sodium ion (MDS4, see Figure 3). This rotameric change appears connected to a rotation of residue Asn280$^{7.45}$ from the initial *g-* rotamer to either trans or *g+* (Figure 3A and C). In contrast, rotamer changes in Tpr246$^{6.48}$ and to a lesser extent Asn280$^{7.45}$ were not observed when the sodium ion was bound to the allosteric site (MDS2), suggesting that the sodium ion contributes to a stabilization of these two residues (Figure 3A and B). Similarly, the furyl moiety of the antagonist ZM-241,385 stabilized the *g+* rotamer of Trp246$^{6.48}$ through Van der Waals interactions (simulations MDS1 and MDS3). Consequently, no movements in this microenvironment occured with ZM-241,385 bound, regardless of the presence of the sodium ion.

The sodium ion binding site in the A_{2A}AR active-like conformation

Analysis of the agonist-bound structures of A_{2A}AR[18, 19] indicates that the activation–related changes in helix VII partially collapse the sodium ion pocket, making it incompatible with ion binding.[22] In order to further evaluate this effect, the sodium ion-water cluster was simulated in the context of the active-like conformation of A_{2A}AR with agonists UK-432,097 (MDS5) or NECA (MDS6), or without any agonist (MDS7, see Table 1). The simulations show that in the active-like state the receptor cannot bind the sodium ion, as evidenced by two alternative events that occur in the early stages of production runs. In the first event, (observed in 1 out of 3 replicas in MDS5, in 2 out of 3 replicas in MDS6, and in all 3 replicas in MDS7) the ion escaped from the proposed binding site. In the alternative event, observed in the remaining simulations, the ion remained in the allosteric binding site, but a conformational change of helix VII occurred, resembling the inactive-like conformation of helix VII observed in all antagonist-bound A_{2A}AR structures. In particular, the region between His278$^{7.43}$ and Asn284$^{7.49}$ undergoes an outward movement driving helix VII apart from helix III and expanding the pocket cavity (Figure 4). In the MDS5 and MDS6 simulations, this rearrangement was also accompanied by a loss of contact between His278$^{7.43}$ and the O2' of the ribose moiety of the agonist, suggesting that sodium ion binding destabilizes activation-related movements and agonist binding. Note that all conformational events described here occurred within the first 5-10 ns of the simulation, justifying that a total simulation time of 40 ns was sufficient to properly sample the sodium binding site in the active-like system. These findings indicate that the

binding of sodium ions and agonists each require a different conformational state of the receptor and, therefore, are mutually exclusive.

A

	MDS2	MDS4
%χ1-$W^{6.48}$ g(+) rotamer	96.8%	38.5%
%χ2-$N^{7.45}$ g(-) rotamer	53.3%	1.0%
Average # water @3Å of $D^{2.50}$	2.7	3.6

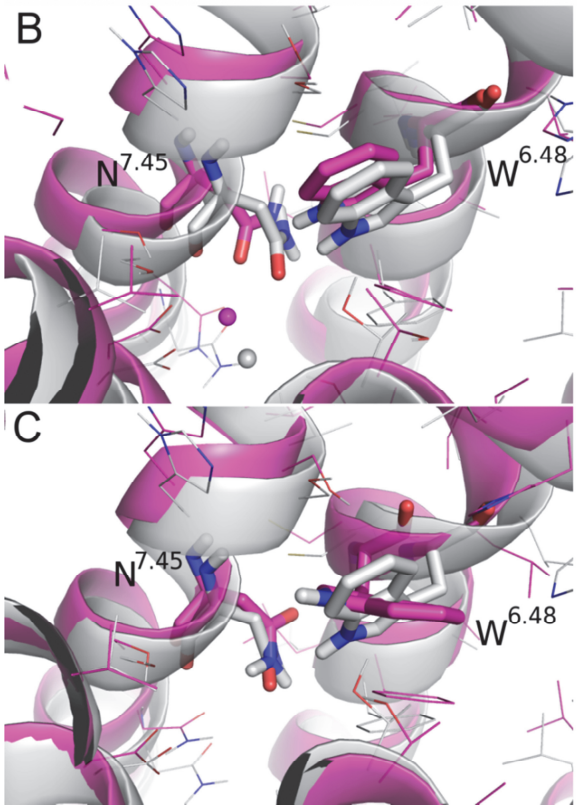

Figure 3. Rotameric transitions of $Trp^{6.48}$ and $Asn^{7.45}$ in the *apo* simulations of the inactive A_{2A}AR. **A)** Populations of the initial conformational states in the simulations with (MDS2) and without (MDS4) the sodium ion, and the number of waters in the ion binding site (each data is an average of the 3 MD replicas). Note that $Trp^{6.48}$ only finds the trans conformation when not in the initial g(+) conformation, while $Asn^{7.45}$ is more flexible and can be found in either trans, g(+) or the initial g(-) conformations. **B)** and **C)** Representative snapshot (magenta) of the conformation of these two residues in MDS2 **(B)** and MDS4 **(C)**, with the reference crystal structure overlaid in light gray.

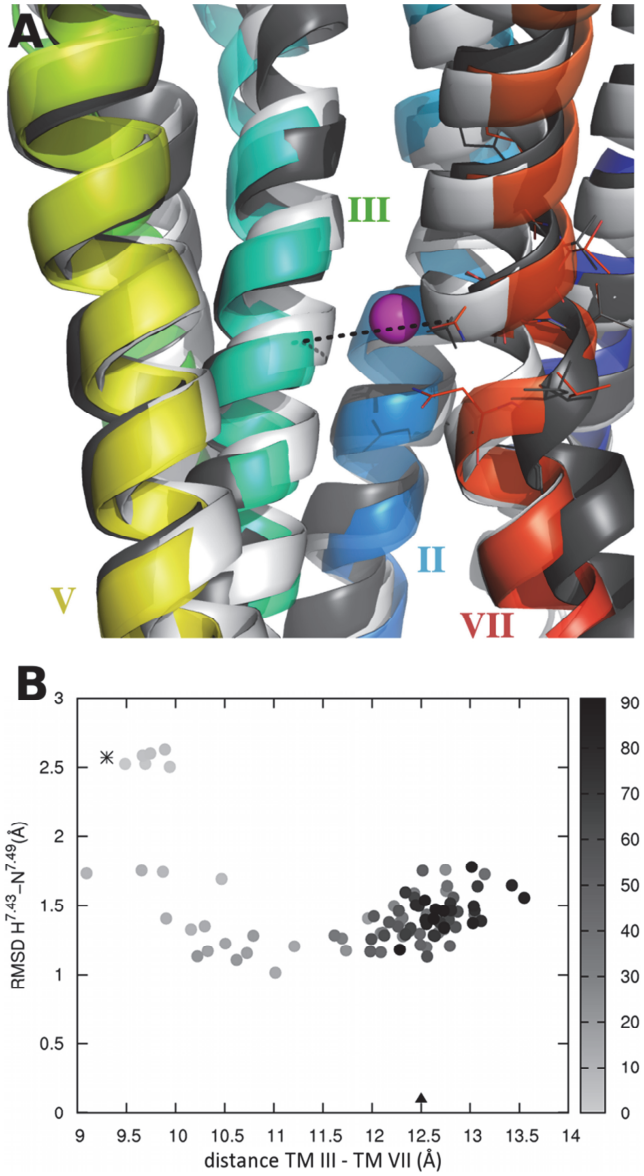

Figure 4. The movement of helix VII in order to accommodate the sodium ion. **A)** Starting (light grey) and ending (rainbow, with helix VII colored orange) conformations of the agonist-bound $A_{2A}AR$ in the presence of sodium ion (MDS5), with the inactive crystal structure denoted in anthracite. **B)** The distance between helices III and VII (X axis, Cα of residues $Ile^{3.40}$ and $Asn^{7.45}$ as indicated by a dashed line in **A**) is plotted against the backbone RMSD of the motif $His^{7.43}$-$Asn^{7.49}$, (Y axis), using as a reference the inactive conformation of $A_{2A}AR$. Each dot is a snapshot extracted every 0.5 ns, with the time evolution depicted by the shading code (light grey -> black). Active and inactive conformations are indicated with an asterisk and a triangle, respectively.

Amiloride and HMA as A_{2A}AR allosteric modulators

Amiloride and its derivatives are known to be nonspecific GPCR modulators.[50] A binding mode of amiloride and its bulkier analog HMA to the A_{2A}AR was determined by flexible side chain docking where the charged guanidinium group of amiloride interacted with Asp52$^{2.50}$.[22] An additional hydrogen bond was also predicted between amiloride and the Trp246$^{6.48}$ side chain (see Figure 5A), which is shifted ~1.5 Å towards the orthosteric pocket as a result of induced fit. This tight binding of amilorides is clearly not compatible with the collapsed allosteric pocket observed in the active-like conformation of the A_{2A}AR, in an even more pronounced way than in the case of sodium ions. Therefore, we explored this docking hypothesis with a series of MD simulations of the inactive A_{2A}AR in the presence of different orthosteric antagonists, i.e. the ternary complexes A_{2A}AR-ZM-241,385-amiloride (MDS8) and A_{2A}AR-caffeine-amiloride (MDS9). The effect of amiloride on the binding of antagonists turned out to be complex and varied between the different antagonist chemotypes tested. Figure 5D shows a comparison of the RMSF (root mean square fluctuation) of compound ZM-241,385 with no allosteric modulator present (MDS3), and with either sodium ion (MDS1), amiloride (MDS8) or HMA (MDS11) present in the proposed allosteric site. A significant increase in the mobility of ZM-241,385 ($p<0.05$) was observed in the presence of both amilorides. This effect is likely due to the influence of the side chain of Trp246$^{6.48}$, which is the only residue that interacts with ZM-241,385 and amilorides simultaneously (in particular with the 5'-azepane substituent of HMA, see Figure 5C), leading to the hypothesis that this highly conserved residue acts as an important link between the two sites. Consequently, binding of antagonists that do not directly interact with Trp246$^{6.48}$, for example, caffeine,[14] should be less affected by the presence of amiloride in the allosteric site (Figure 5B). Indeed, we found no statistically significant difference for the mobility of caffeine as a function of the presence of amilorides (Figure 5D). Due to the high mobility of caffeine, which is small in size, has few receptor contacts, and displays low affinity, the simulation time in this particular system was limited to 40 ns time scale.

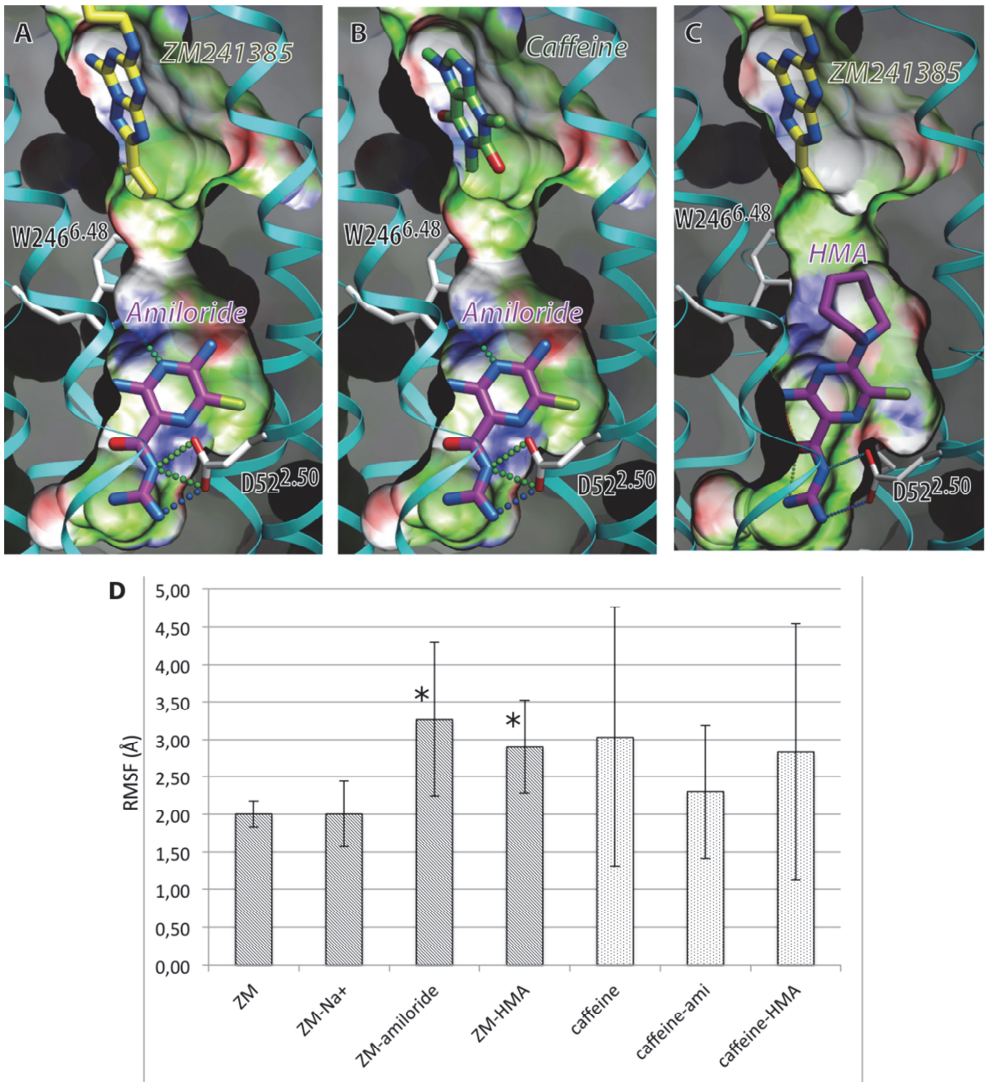

Figure 5. Impact of amiloride and HMA on binding of antagonists. **A)** Amiloride docking (magenta carbons) induces a shifted position of Trp246$^{6.48}$ side chain, revealing potential steric clashes with the orthosteric ligand ZM-241,385 (yellow carbons, superimposed from the crystal structure with PDB code 4EIY). **B)** Same conformation of the amiloride-bound A_{2A}AR, with the caffeine pose (green carbons) superimposed from the crystal structure of A_{2A}AR/caffeine complex (PDB code 3RFM). **C)** Flexible docking of HMA (magenta carbons) is predicted to further shift Trp246$^{6.48}$ and interfere with ZM-241,385 binding. **D)** Mobility of antagonists in presence or absence of amiloride, HMA and the sodium ion in the allosteric pocket, calculated as RMSF from the MD simulations (dark shaded bars for ZM-241,385; light shaded bars for caffeine). Error bars indicate the standard deviation estimated from three MD replicas (n=3); ami=amiloride; ZM= ZM-241,385. Significantly different from the control simulation (absence of any allosteric ligand) in a Student's t-test with *$p < 0.05$.

Biochemical studies

Radioligand binding experiments were performed to examine the effects of sodium ions and amiloride derivatives on antagonist, [^{3}H]ZM-241,385, and agonist, [^{3}H]NECA, binding to the A_{2A}AR. In order to experimentally assess the dependence of ligand binding on the presence of a sodium ion in the allosteric site, we performed equilibrium displacement studies with increasing concentrations of NaCl (Figure 6A). These experiments show a full displacement of [^{3}H]NECA by sodium ions, with an IC_{50} value of 49 ± 7 mM (Table S2 and Figure 6A). In contrast, there is an enhancement of antagonist [^{3}H]ZM-241,385 binding, especially at higher sodium ion concentrations. All these results correlate with the MD conclusions that the sodium ion selectively stabilizes the antagonist-bound receptor state.

Saturation binding experiments performed with [^{3}H]NECA also show that the presence of NaCl significantly reduces [^{3}H]NECA binding to the A_{2A}AR (Table 2 and Figure S3). Interestingly, this reduction in agonist binding was due to an increase of the K_D value while the radioligand's B_{max} value remained at a control level, within experimental error. This profile of pharmacological parameters usually implies a competitive interaction between the two ligands. However, in this case the binding sites of the two ligands are not overlapping, therefore the observed "mutually exclusive binding" suggests that the sodium ion-bound conformation of A_{2A}AR is not compatible with agonist binding, and vice-versa. In contrast, no significant effect of sodium ions was observed on the binding of the antagonist radioligand [^{3}H]ZM-241,385 to the A_{2A}AR (Table 2).

We also characterized the influence of amiloride and HMA on radioligand binding to the A_{2A}AR. The two compounds inhibited the binding of both agonist and antagonist radioligands in displacement assays, albeit with different potencies (Figure 6B and 6C and Table S2). HMA proved to be more active than amiloride in both cases, and displayed the highest potency (2.4 μM) with the agonist [^{3}H]NECA as the radiolabel. Radioligand saturation experiments were performed in the presence of the amiloride analogs, revealing distinct differences between the two radioligands (Table 2 and Figure S3). The interaction between amiloride and [^{3}H]ZM-241,385 was noncompetitive in nature as the radioligand's B_{max} value was significantly reduced with little effect on the K_D value, whereas unlabeled ZM-241,385, serving as a control orthosteric ligand, showed all traits of a competitive ligand. In this experimental setup, HMA behaved somewhat in between ZM-241,385 and amiloride, showing a small but significant shift in K_D and a nonsignificant

change in B_{max} value. Similar experiments with the radiolabeled agonist [^{3}H]NECA produced a very different outcome. While unlabeled ZM-241,385 appeared competitive with [^{3}H]NECA, as expected for two orthosterically binding compounds, the same was true for the interaction between the amilorides and [^{3}H]NECA. Hardly any effect was observed on NECA's B_{max} value, whereas all K_D values were significantly increased, which we attribute to the mechanism of "mutually exclusive binding" discussed above for the case of agonist and sodium ion binding.

Table 2. Saturation of [^{3}H]ZM-241,385 and NECA spiked with 25% [^{3}H]NECA binding to human A_{2A}ARs transiently expressed in HEK293T cell membranes in the absence and presence of ZM-241,385, NaCl, amiloride, and HMA. See associated experiments in Figure S3.

	[^{3}H]ZM-241,385		[^{3}H]NECA	
	K_D (nM)	**B_{max}[a] (%)**	**K_D (nM)**	**B_{max}[a] (%)**
Control	1.3 ± 0.4	100 ± 10	84 ± 11	100 ± 2
+ 10 nM ZM	8.3 ± 2.2**	85 ± 7	123 ± 9*	95 ± 3
+ 30 mM NaCl	1.2 ± 0.3	120 ± 11	213 ± 10***	106 ± 4
+ 100 mM NaCl	0.8 ± 0.1	87 ± 3	471 ± 53***	114 ± 9
+ 30 µM Amiloride	1.9 ± 0.8	61 ± 4*	290 ± 52**	119 ± 13
+ 3 or 4 µM HMA[b]	4.1 ± 0.9*	78 ± 9	246 ± 2***	110 ± 1*

a: % of Bmax of control (= 100%)
b: 3 µM HMA for [3H]ZM-241,385 and 4 µM HMA for [3H]NECA
Significantly different from control in a Student's t-test with * $p < 0.05$, ** $p < 0.01$, or *** $p < 0.001$. Values are means ± SEM of 2-5 separate assays performed in duplicate.

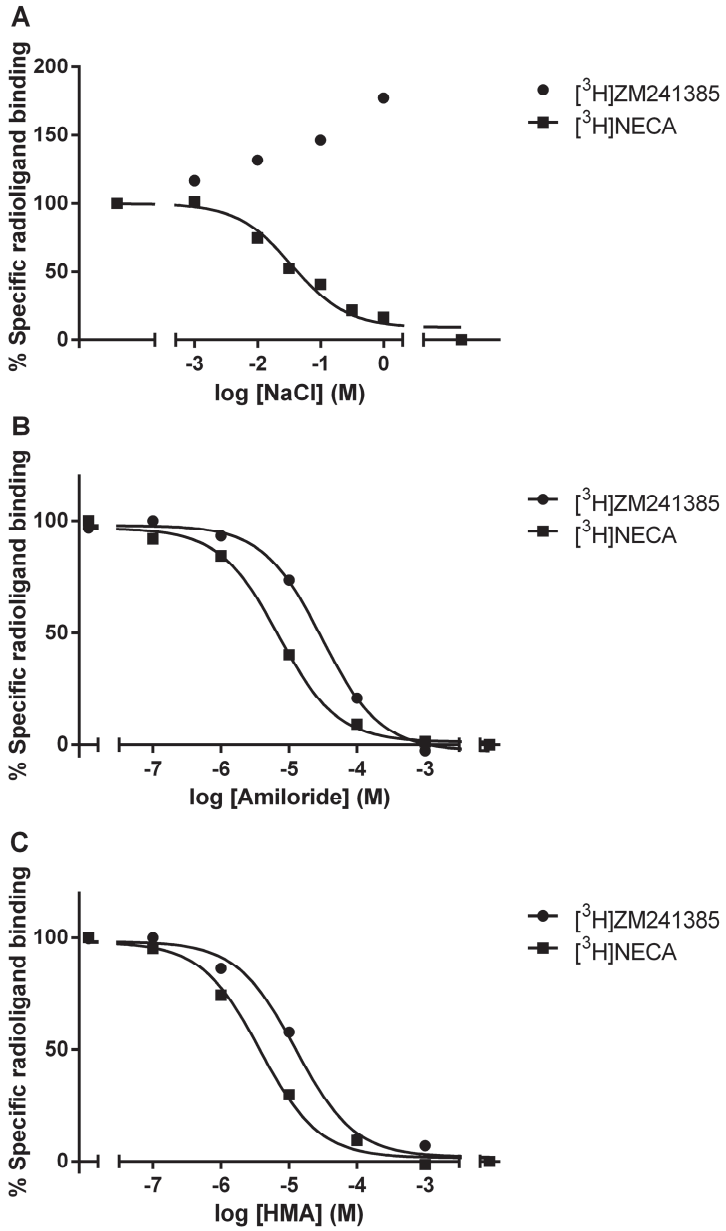

Figure 6. Equilibrium displacement of [^{3}H]ZM-241,385 and [^{3}H]NECA by allosteric modulators. NaCl **(A)**, amiloride **(B)**, and HMA **(C)**. Representative graphs from one experiment performed in duplicate on hA_{2A}ARs transiently expressed in HEK293T cell membranes. Associated IC_{50} values listed in Table S2.

Biophysical studies

The effects of sodium ions, orthosteric ligands and amiloride analogs on A_{2A}AR stability were analyzed with a series of thermal stability assays.[48] Increasing sodium ion concentrations induced a significant increase in the thermostability of the unliganded A_{2A}AR-BRIL complex, as shown in Figure 7A. A two-phase response was observed, with a modest increase in thermostability from 52 to 57 °C at sodium ion concentrations below the physiological concentration of 150 mM, and a further more substantial increase to 65 °C upon addition of higher concentrations up to 500 mM NaCl.

In order to evaluate the effects of allosteric modulators on various receptor-ligand complexes, we measured the thermal stability of the A_{2A}AR-BRIL construct in the presence or absence of sodium ions and/or amiloride, and their combinations with the orthosteric ligands caffeine (antagonist), ZM-241,385 (antagonist), or UK-432,097 (full agonist) (Figure 7B). Sodium ions and amiloride each increased A_{2A}AR thermostability by 5-6 °C, but their effect when combined was non-additive, corroborating the suggested competition of these two charged molecules for the same binding site. In contrast, the addition of caffeine in the presence of saturating concentrations of amiloride or sodium ions caused a further 6 °C increase in the thermostability of the complex, suggesting an additive stabilizing effect of the orthosteric caffeine and allosteric ligands. Also, while we observed an additive effect of sodium ions and ZM-241,385, amiloride did not contribute to the stability of A_{2A}AR in saturating concentrations of ZM-241,385, in agreement with unfavorable indirect interactions between amiloride and ZM-241,385. Finally, neither sodium ions nor amiloride had a stabilizing effect on the A_{2A}AR saturated with UK-432,097, likely because this agonist precluded binding of these allosteric modulators.

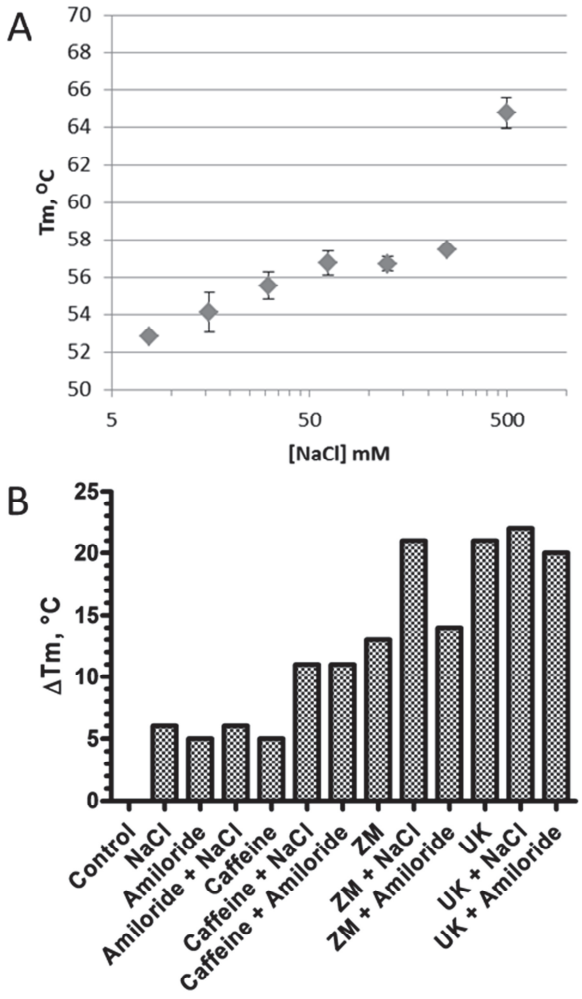

Figure 7. Effect of allosteric binders on A_{2A}AR thermostability measured by CPM assays. **A)** Effect of titration of NaCl on A_{2A}AR thermostability, mean ± SEM shown for measurements performed in triplicate. **B)** Effect of NaCl (150 mM), amiloride (100 µM), caffeine (500 µM), ZM-241,385 (50 µM), UK-432,097 (50 µM) and combinations thereof on A_{2A}AR thermostability.

Discussion

The 1.8 Å resolution structure of A_{2A}AR in complex with the antagonist ZM-241,385 revealed a highly conserved sodium ion binding site[22] and provided an excellent opportunity to examine the molecular mechanism of the allosteric modulation of sodium ions in this receptor. Our MD simulations suggest that the electron density assigned to the water molecule closest to sodium ion in the crystal structure (W52) could correspond to a second resonance position of the ion, which would involve direct interaction with another conserved residue, Asn280$^{7.45}$ (Figure 2). Although we could not find a clear evidence of such dynamic rearrangements in the A_{2A}AR crystal structure, this may reflect the "frozen" state of the sodium ion-water cluster at the low temperatures (~100K) used in cryo-crystallography. While further crystallographic studies at room temperature may help to validate such subtle effects experimentally,[51] the thermal fluctuations explored by the MD simulations under physiological conditions are particularly suited to explore this phenomenon.[52] The potential dynamic nature of the sodium ion and water network in the allosteric pocket could partially explain why the ion was not observed previously in lower resolution GPCR structures. A closer look at this region in two recently published, antagonist-bound GPCR structures, i.e. carvedilol-β_1-adrenergic receptor[53] and βFNA-μ opioid receptor,[54] reveals that they are indeed compatible with the presence of a sodium ion (Figure S1). More recently, a similar configuration of the sodium ion/water network was also identified in other ligand complexes of the β_1-adrenergic receptor.[55]

The communication between the highly conserved class A GPCR residues Asp$^{2.50}$, Trp$^{6.48}$, and to a lesser extent Asn$^{7.45}$, had been suggested to occur through a cluster of water molecules.[24] The current MD results strongly support the preference of the sodium ion for the inactive conformation of this micro-environment, at least in the A_{2A}AR, suggesting that it contributes to its stabilization. The increased dynamic flexibility of Trp246$^{6.48}$ and Asn280$^{7.45}$ in the absence of the sodium ion (Figure 3) is consistent with previous MD simulations of the A_{2A}AR,[37] and agrees well with similar MD simulations in the dopamine D_2 receptor with explicit consideration of a sodium ion.[27] The conformational flexibility of Trp$^{6.48}$ has been associated with the initial steps of the activation mechanism of GPCRs,[56, 57] probably by facilitating the higher order conformational changes observed in helix VI between inactive and active states. Conversely, the presence of the sodium ion and coordinating water molecules in this

pocket hampers an activation-related inward movement of helix VII towards helix III,[18, 19] as indicated by MD simulations. Instead, we observed an "inactivation" movement of helix VII in the agonist-bound conformation (Figure 4) that led to the loss of key agonist-receptor interactions, suggesting that the simultaneous binding of the allosteric ion and the orthosteric agonist to the same receptor molecule is unlikely. Such a structural mechanism explains the negative allosteric effect of sodium ions on agonist binding to the A_{2A}AR observed here (Figure 6A and Table 2) and in earlier studies.[6, 22]

In radioligand binding experiments performed with both agonist and antagonist radioligands, sodium ions differentially affected radioligand binding to the A_{2A}AR, providing further insights into its allosteric effect: they induced an increase in [^{3}H]ZM-241,385 binding, but abrogated [^{3}H]NECA binding in a concentration-dependent manner with an IC_{50} value of approximately 50 mM (Figure 6A). This potency is in the same range of sodium ion concentrations that cause an increase in receptor thermostability (Figure 7), indicating that sodium ion binding could mediate both effects. Moreover, this IC_{50} corresponds to about one third of the extracellular physiological concentration of sodium ions. This suggests that about 75% of the A_{2A}ARs that are present in the body are in a sodium ion occupied state, provided that there is unrestricted access to the sodium binding site from the outside of the cell, as recently proposed for the dopamine D_2 receptor.[27] Thus, it is likely that sodium is significantly involved in modulating the physiological state of the A_{2A}AR and possibly other class A GPCRs.

Interestingly, saturation binding experiments (Table 2) demonstrate that the presence of sodium ions (30 and 100 mM) reduces [^{3}H]NECA affinity (K_D) rather than its B_{max} value, while no affinity reduction was observed for [^{3}H]ZM-241,385. This fact, together with the observed increase of [^{3}H]ZM-241,385 binding at high sodium ion concentrations (Figure 6A), is in good agreement with an earlier study where the slight affinity increase of this radioligand at even higher sodium concentrations (1 M)[58] was due to a decrease in its dissociation rate.[6] The structural information and the computational results provided in this study suggest that binding of agonists and sodium ions can be considered as "mutually exclusive".[59] This mechanism is further supported by thermal stability assays, showing that antagonists ZM-241,385 and caffeine display additive stabilizing effects with sodium ions, whereas the agonist UK-432,097 stabilizes the receptor but shows no additive effect when any allosteric ligand is added (Figure 7B).

Similar to sodium ions, the diuretic drug amiloride is an allosteric modulator of several GPCRs (Chapter 2), including such diverse subfamilies as adenosine, aminergic and gonadotropin-releasing hormone receptors.[6, 60-64] The present study in the human A_{2A}AR shows that both amiloride and its derivative HMA negatively modulate agonist binding (Table 2), with HMA being more potent than amiloride in radioligand displacement studies (Figure 6) as previously suggested by kinetic studies in the rat A_{2A}AR.[6] The saturation studies with [^{3}H]ZM-241,385 as the radioligand (Table 2) also point to a noncompetitive interaction between amiloride and the antagonist binding site. Moreover, the additive increase in A_{2A}AR thermostability in the presence of both amiloride and the orthosteric antagonist caffeine (Figure 7B) suggests that both allosteric and orthosteric ligands can bind simultaneously. These findings are in concert with docking and MD simulations (Figure 5), which suggest that amiloride and HMA bind in the allosteric sodium pocket, with the charged guanidinium group anchored by the carboxyl of Asp$^{2.50}$. Although the proposed amiloride binding does not directly overlap with the orthosteric ligand binding site, our simulations indicate that amiloride derivatives can impact orthosteric ligand binding indirectly, primarily via modulation of Trp246$^{6.48}$ conformation. This explains a more pronounced negative allosteric effect of HMA, which has extensive steric interactions with the Trp246$^{6.48}$ side chain. Overall, the distinct allosteric effects of amilorides are probably the result of a delicate balance between an improved stability of the inactive conformation and an indirect (noncompetitive) interference with the orthosteric site for antagonists.

In summary, a combination of biochemical and thermal stability data with MD simulations, based on both inactive and the active-like crystal structures of the A_{2A}AR, provided valuable mechanistic insights into the role of the allosteric sodium ion in the conformational equilibrium of the receptor. Our findings suggest that the binding of either the sodium ion or amilorides to the allosteric pocket selectively stabilizes the inactive conformation of the receptor, and this allosteric effect is responsible for the observed reduction in orthosteric agonist binding. Comprehensive experimental and theoretical analyses of A_{2A}AR in simultaneous complex with both allosteric modulators and orthosteric ligands also explain, on a molecular basis, the distinct interaction profiles observed between allosteric amiloride derivatives and different orthosteric antagonists. These observations pave the way for better understanding of GPCR allosteric control,

which may be used in the design of novel allosteric modulators to more precisely tune receptor function.

Supplemental information

Supplemental information includes supplemental experimental procedures, Figures S1-S3, and Tables S1 and S2, and can be found with this article online at dx.doi.org/10.1016/ j.str.2013.09.020

Acknowledgements

This work was supported by NIGMS PSI:Biology grant U54 GM094618 (R.C.S., V.K., V.C.). H.G.T. acknowledges the Spanish Ministry of Education for the mobility program (JC2011-0387) and financial support from the Spanish National Plan for R+D (SAF2011-30104). L.H.H., A.P.IJ. and A.M. thank the Dutch Research Council (NWO) for financial support (NWO-TOP #714.011.001 and NWO-Veni #11188).

References

1. Christopoulos A, *Allosteric binding sites on cell-surface receptors: novel targets for drug discovery.* Nat Rev Drug Discov, 2002. 1(3): p. 198-210.
2. Conn PJ, Christopoulos A, and Lindsley CW, *Allosteric modulators of GPCRs: a novel approach for the treatment of CNS disorders.* Nat Rev Drug Discov, 2009. 8(1): p. 41-54.
3. Gao ZG and Jacobson KA, *Keynote review: allosterism in membrane receptors.* Drug Discov Today, 2006. 11(5-6): p. 191-202.
4. Göblyös A and IJzerman AP, *Allosteric modulation of adenosine receptors.* Biochim Biophys Acta, 2011. 1808(5): p. 1309-18.
5. Jacobson KA, Gao ZG, Goblyos A, et al., *Allosteric modulation of purine and pyrimidine receptors.* Adv Pharmacol, 2011. 61: p. 187-220.
6. Gao ZG and IJzerman AP, *Allosteric modulation of A_{2A} adenosine receptors by amiloride analogues and sodium ions.* Biochem Pharmacol, 2000. 60(5): p. 669-76.
7. Neve KA, Cumbay MG, Thompson KR, et al., *Modeling and mutational analysis of a putative sodium-binding pocket on the dopamine D_2 receptor.* Mol Pharmacol, 2001. 60(2): p. 373-81.
8. Rosenbaum DM, Cherezov V, Hanson MA, et al., *GPCR engineering yields high-resolution structural insights into β_2-adrenergic receptor function.* Science, 2007. 318(5854): p. 1266-73.
9. Cherezov V, *Lipidic cubic phase technologies for membrane protein structural studies.* Curr Opin Struct Biol, 2011. 21(4): p. 559-66.
10. Tate CG and Schertler GF, *Engineering G protein-coupled receptors to facilitate their structure determination.* Curr Opin Struct Biol, 2009. 19(4): p. 386-95.
11. Katritch V, Cherezov V, and Stevens RC, *Structure-function of the G protein-coupled receptor superfamily.* Annu Rev Pharmacol Toxicol, 2013. 53: p. 531-56.
12. Congreve M, Langmead CJ, Mason JS, et al., *Progress in structure based drug design for G protein-coupled receptors.* J Med Chem, 2011. 54(13): p. 4283-311.

13. Dror RO, Arlow DH, Borhani DW, et al., *Identification of two distinct inactive conformations of the β2-adrenergic receptor reconciles structural and biochemical observations.* Proc Natl Acad Sci USA, 2009. 106(12): p. 4689-94.
14. Dore AS, Robertson N, Errey JC, et al., *Structure of the adenosine A_{2A} receptor in complex with ZM241385 and the xanthines XAC and caffeine.* Structure, 2011. 19(9): p. 1283-93.
15. Jaakola VP, Griffith MT, Hanson MA, et al., *The 2.6 Ångstrom crystal structure of a human A_{2A} adenosine receptor bound to an antagonist.* Science, 2008. 322(5905): p. 1211-7.
16. Congreve M, Andrews SP, Dore AS, et al., *Discovery of 1,2,4-triazine derivatives as adenosine A_{2A} antagonists using structure based drug design.* J Med Chem, 2012. 55(5): p. 1898-903.
17. Hino T, Arakawa T, Iwanari H, et al., *G-protein-coupled receptor inactivation by an allosteric inverse-agonist antibody.* Nature, 2012. 482(7384): p. 237-40.
18. Lebon G, Warne T, Edwards PC, et al., *Agonist-bound adenosine A_{2A} receptor structures reveal common features of GPCR activation.* Nature, 2011. 474(7352): p. 521-5.
19. Xu F, Wu H, Katritch V, et al., *Structure of an agonist-bound human A_{2A} adenosine receptor.* Science, 2011. 332(6027): p. 322-7.
20. Rasmussen SG, DeVree BT, Zou Y, et al., *Crystal structure of the β2 adrenergic receptor-G_s protein complex.* Nature, 2011. 477(7366): p. 549-55.
21. Park JH, Scheerer P, Hofmann KP, et al., *Crystal structure of the ligand-free G-protein-coupled receptor opsin.* Nature, 2008. 454(7201): p. 183-7.
22. Liu W, Chun E, Thompson A, et al., *Structural basis for allosteric regulation of GPCRs by sodium ions.* Science, 2012. 337: p. 232-6.
23. Mirzadegan T, Benko G, Filipek S, et al., *Sequence analyses of G-protein-coupled receptors: Similarities to rhodopsin.* Biochemistry, 2003. 42(10): p. 2759-67.
24. Pardo L, Deupi X, Dölker N, et al., *The role of internal water molecules in the structure and function of the rhodopsin family of G protein-coupled receptors.* Chembiochem, 2007. 8(1): p. 19-24.
25. Angel TE, Chance MR, and Palczewski K, *Conserved waters mediate structural and functional activation of family A (rhodopsin-like) G protein-coupled receptors.* Proc Natl Acad Sci USA, 2009. 106(21): p. 8555-60.
26. Barbhaiya H, McClain R, IJzerman A, et al., *Site-directed mutagenesis of the human A_1 adenosine receptor: influences of acidic and hydroxy residues in the first four transmembrane domains on ligand binding.* Mol Pharmacol, 1996. 50(6): p. 1635-42.
27. Selent J, Sanz F, Pastor M, et al., *Induced effects of sodium ions on dopaminergic G-protein coupled receptors.* PLoS Comput Biol, 2010. 6(8): p. e1000884.
28. Pert CB, Pasternak G, and Snyder SH, *Opiate agonists and antagonists discriminated by receptor binding in brain.* Science, 1973. 182(4119): p. 1359-61.
29. Snyder SH and Pasternak GW, *Historical review: Opioid receptors.* Trends Pharmacol Sci, 2003. 24(4): p. 198-205.
30. Tsai BS and Lefkowitz RJ, *Agonist-specific effects of monovalent and divalent cations on adenylate cyclase-coupled α adrenergic receptors in rabbit platelets.* Mol Pharmacol, 1978. 14(4): p. 540-8.
31. Horstman DA, Brandon S, Wilson AL, et al., *An aspartate conserved among G-protein receptors confers allosteric regulation of α_2-adrenergic receptors by sodium.* J Biol Chem, 1990. 265(35): p. 21590-5.
32. Proulx CD, Holleran BJ, Boucard AA, et al., *Mutational analysis of the conserved Asp2.50 and ERY motif reveals signaling bias of the urotensin II receptor.* Mol Pharmacol, 2008. 74(3): p. 552-61.

33. Gao ZG, Kim SK, Gross AS, et al., *Identification of essential residues involved in the allosteric modulation of the human A_3 adenosine receptor.* Mol Pharmacol, 2003. 63(5): p. 1021-31.
34. Nie J and Lewis DL, *Structural domains of the CB_1 cannabinoid receptor that contribute to constitutive activity and G-protein sequestration.* J Neurosci, 2001. 21(22): p. 8758-64.
35. Ballesteros JA and Weinstein H, *Integrated methods for the construction of three dimensional models and computational probing of structure-function relations in G-protein coupled receptors*, in *Methods Neurosci*. 1995, Academic Press: San Diego. p. 366-428.
36. Hess B, Kutzner C, Van der Spoel D, et al., *GROMACS 4: Algorithms for highly efficient, load-balanced, and scalable molecular simulation.* J Chem Theory Comput, 2008. 4(3): p. 435-47.
37. Rodríguez D, Piñeiro A, and Gutiérrez-de-Terán H, *Molecular dynamics simulations reveal insights into key structural elements of adenosine receptors.* Biochemistry, 2011. 50(19): p. 4194-08.
38. Gutierrez-de-Teran H, Bello X, and Rodriguez D, *Characterization of the dynamic events of GPCRs by automated computational simulations.* Biochem Soc Trans, 2013. 41(1): p. 205-12.
39. Kaminski GA, Friesner RA, Tirado-Rives J, et al., *Evaluation and reparametrization of the OPLS-AA force field for proteins via comparison with accurate quantum chemical calculations on peptides.* J Phys Chem B, 2001. 105(28): p. 6474-87.
40. Schrödinger LLC, *Macromodel, version9.7*. 2009: New York, NY.
41. Berger O, Edholm O, and Jähnig F, *Molecular dynamics simulations of a fluid bilayer of dipalmitoylphosphatidylcholine at full hydration, constant pressure, and constant temperature.* Biophys J, 1997. 72(5): p. 2002-13.
42. Chakrabarti N, Neale C, Payandeh J, et al., *An iris-like mechanism of pore dilation in the CorA magnesium transport system.* Biophys J, 2010. 98(5): p. 784-92.
43. Berendsen HJC, Postma JPM, Van Gunsteren WF, et al., *Interaction models for water in relation to protein hydration*, in *Intermolecular Forces*, 1981, Dordrecht: D. Reidel Publishing Company. p. 331-42.
44. Nose S and Klein ML, *Constant pressure molecular-dynamics for molecular-systems.* Mol Phys, 1983. 50(5): p. 1055-76.
45. Humphrey W, Dalke A, and Schulten K, *VMD - Visual molecular dynamics.* J Mol Graphics, 1996. 14: p. 33-8.
46. Sambrook J and Fritsch EF, *Molecular Cloning: A Laboratory Manual*. 2nd ed. 1989, Cold Spring Harbor, NY: Cold Spring Harbor Laboratory.
47. Smith PK, Krohn RI, Hermanson GT, et al., *Measurement of protein using bicinchoninic acid.* Anal Biochem, 1985. 150(1): p. 76-85.
48. Alexandrov AI, Mileni M, Chien EY, et al., *Microscale fluorescent thermal stability assay for membrane proteins.* Structure, 2008. 16(3): p. 351-9.
49. Harding MM, *Small revisions to predicted distances around metal sites in proteins.* Acta Crystallogr D, 2006. 62: p. 678-82.
50. Garritsen A, IJzerman AP, Tulp MTM, et al., *Receptor binding profiles of amiloride analogues provide no evidence for a link between receptors and the Na^+/H^+ exchanger, but indicate a common structure on receptor proteins.* J Recept Res, 1991. 11(6): p. 891-907.
51. Fraser JS, Van den Bedem H, Samelson AJ, et al., *Accessing protein conformational ensembles using room-temperature X-ray crystallography.* Proc Natl Acad Sci USA, 2011. 108(39): p. 16247-52.
52. Ulmschneider MB, Bagneris C, McCusker EC, et al., *Molecular dynamics of ion transport through the open conformation of a bacterial voltage-gated sodium channel.* Proc Natl Acad Sci USA, 2013. 110(16): p. 6364-9.

53. Warne T, Edwards PC, Leslie AG, et al., *Crystal structures of a stabilized β_1-adrenoceptor bound to the biased agonists bucindolol and carvedilol.* Structure, 2012. 20(5): p. 841-9.
54. Manglik A, Kruse AC, Kobilka TS, et al., *Crystal structure of the μ-opioid receptor bound to a morphinan antagonist.* Nature, 2012. 485(7398): p. 321-6.
55. Christopher JA, Brown J, Dore AS, et al., *Biophysical fragment screening of the β_1-adrenergic receptor: identification of high affinity arylpiperazine leads using structure-based drug design.* J Med Chem, 2013. 56(9): p. 3446-55.
56. Schwartz TW, Frimurer TM, Holst B, et al., *Molecular mechanism of 7TM receptor activation--a global toggle switch model.* Annu Rev Pharmacol Toxicol, 2006. 46: p. 481-519.
57. Shi L and Javitch JA, *The binding site of aminergic G protein-coupled receptors: the transmembrane segments and second extracellular loop.* Annu Rev Pharmacol Toxicol, 2002. 42: p. 437-67.
58. Gao ZG, Jiang Q, Jacobson KA, et al., *Site-directed mutagenesis studies of human A_{2A} adenosine receptors: involvement of Glu^{13} and His^{278} in ligand binding and sodium modulation.* Biochem Pharmacol, 2000. 60(5): p. 661-8.
59. Neubig RR, Spedding M, Kenakin T, et al., *International Union of Pharmacology Committee on Receptor Nomenclature and Drug Classification. XXXVIII. Update on terms and symbols in quantitative pharmacology.* Pharmacol Rev, 2003. 55(4): p. 597-606.
60. Heitman LH, Ye K, Oosterom J, et al., *Amiloride derivatives and a nonpeptidic antagonist bind at two distinct allosteric sites in the human gonadotropin-releasing hormone receptor.* Mol Pharmacol, 2008. 73(6): p. 1808-15.
61. Gao ZG, Melman N, Erdmann A, et al., *Differential allosteric modulation by amiloride analogues of agonist and antagonist binding at A_1 and A_3 adenosine receptors.* Biochem Pharmacol, 2003. 65(4): p. 525-34.
62. Hoare SR, Coldwell MC, Armstrong D, et al., *Regulation of human D_1, $D_{2(long)}$, $D_{2(short)}$, D_3 and D_4 dopamine receptors by amiloride and amiloride analogues.* Br J Pharmacol, 2000. 130(5): p. 1045-59.
63. Pauwels PJ, *Competitive and silent antagonism of recombinant 5-HT_{1B} receptors by amiloride.* Gen Pharmacol, 1997. 29(5): p. 749-51.
64. Howard MJ, Hughes RJ, Motulsky HJ, et al., *Interactions of amiloride with α- and β-adrenergic receptors: amiloride reveals an allosteric site on α_2-adrenergic receptors.* Mol Pharmacol, 1987. 32(1): p. 53-8.